equation in the Lab, $\boldsymbol{p}_1 = \boldsymbol{q}_1 + \boldsymbol{q}_2$. Any desired relation between momenta, energies or angles may be extracted from this diagram without difficulty. We consider explicitly only a few important relations.

By (7.18), the vectors $\boldsymbol{p}^*, \boldsymbol{q}^*, \boldsymbol{q}_2$ form an isosceles triangle. Thus the recoil angle and the magnitude of the recoil momentum q_2 are given in terms of CM quantities by

$$\alpha = \tfrac{1}{2}(\pi - \theta^*), \qquad q_2 = 2p^* \sin \tfrac{1}{2}\theta^*. \tag{7.21}$$

The Lab kinetic energy transferred to the target particle is therefore

$$T_2 = \frac{q_2^2}{2m_2} = \frac{2p^{*2}}{m_2} \sin^2 \tfrac{1}{2}\theta^*.$$

On the other hand, the total kinetic energy in the Lab is just the kinetic energy of the incoming particle,

$$T = \frac{p_1^2}{2m_1} = \frac{M^2 p^{*2}}{2m_1 m_2^2},$$

by (7.20). The interesting quantity is the fraction of the total kinetic energy which is transferred. This is

$$\frac{T_2}{T} = \frac{4m_1 m_2}{M^2} \sin^2 \tfrac{1}{2}\theta^*. \tag{7.22}$$

The maximum possible kinetic energy transfer occurs for a head-on collision ($\theta^* = \pi$), and is $T_2/T = 4m_1 m_2/(m_1 + m_2)^2$. Clearly this can be close to unity only if m_1 and m_2 are comparable in magnitude. If the incoming particle is very light, it bounces off the target with little loss of energy; if it is very heavy, it is hardly deflected at all from its original trajectory, and again loses little of its energy. For example, in a proton–α-particle collision ($m_1/m_2 = 4$ or $\frac{1}{4}$), the maximum fractional energy transfer is 64 per cent. In an electron–proton collision ($m_1/m_2 = 1/1836$) it is about 0.2 per cent. (These conclusions are changed by relativistic effects for speeds approaching that of light.)

Another important relation is that between the Lab and CM scattering angles. It is easy to prove by elementary trigonometry (most simply by dropping a perpendicular from the upper vertex in Fig. 7.5) that

$$\tan\theta = \frac{\sin\theta^*}{(m_1/m_2) + \cos\theta^*}. \tag{7.23}$$

seriously affected by which target particle is struck. We also suppose that the beam is a parallel beam of particles, each with the same mass and velocity, with a particle flux of f particles crossing unit area per unit time.

The incident particles may or may not be the same as those in the target, but for the moment we shall assume that they can be distinguished, so that it is possible to set up a detector to count the number of scattered particles emerging in some direction, without including also the recoiling target particles.

We can now introduce the concept of differential cross-section, just as we did for the case of a fixed target in §4.5. Indeed the fact that the particles that are struck recoil out of the target makes no essential difference. In any one collision, the scattering angle θ will be determined in some way (depending on the shape of the particles) by the impact parameter b. Thus the particles scattered through angles between θ and $\theta + \mathrm{d}\theta$ will be those of the incident particles which strike any one of the target particles with impact parameters between the corresponding values b and $b + \mathrm{d}b$. To find the number emerging within a solid angle in some specified direction, we have to calculate the corresponding cross-sectional area of the incident beam,

$$\mathrm{d}\sigma = b\,|\mathrm{d}b|\,\mathrm{d}\varphi. \tag{7.26}$$

(compare (4.39) and Fig. 4.9), and multiply by the number of target particles, N, and by the flux, f.

If we set up a detector of cross-sectional area $\mathrm{d}A$ at a large distance L from the target, the rate of detection will be

$$\mathrm{d}w = Nf\frac{\mathrm{d}\sigma}{\mathrm{d}\Omega}\frac{\mathrm{d}A}{L^2}, \tag{7.27}$$

exactly as in (4.44). The ratio $\mathrm{d}\sigma/\mathrm{d}\Omega$ is the *Lab differential cross-section.*

We shall return to the question of calculating the Lab differential cross-section later. First, however, we wish to discuss a slightly different type of experiment.

Let us imagine two beams of particles approaching from opposite directions — a 'colliding-beam' experiment. In particular, we shall be interested in the case where the momenta of the particles in the two beams are equal and opposite, so that we are directly concerned with the CM frame. To be specific, let us suppose that the particles in one beam are hard spheres of radius a_1 and those in the other beam are hard spheres of radius a_2. Evidently, a particular pair of particles will collide if the distance b between

We assumed at the beginning of this section that the target particles and beam particles were distinguishable, and that the aim of the experiment was to count scattered beam particles only. However, it is easy to relax this condition. We shall now calculate the rate at which recoiling target particles enter the detector. In a collision in which the incoming particle has impact parameter b, and is moving in a plane specified by the angle φ, the target particle will emerge in a direction specified by the polar angles α, ψ, where α is related to θ^* or b by (7.21) and $\psi = \pi + \varphi$. The number of target particles emerging within the angular range $\mathrm{d}\alpha, \mathrm{d}\psi$ is therefore equal to the number of incident particles in the corresponding range $\mathrm{d}b, \mathrm{d}\varphi$. To determine the number of recoiling particles entering the detector, we have to relate $\mathrm{d}\sigma$ to the solid angle

$$\mathrm{d}\Omega_2 = \sin\alpha \, \mathrm{d}\alpha \, \mathrm{d}\psi.$$

By (7.21), we have $\cos\theta^* = 1 - 2\cos^2\alpha$, whence

$$\frac{\mathrm{d}\sigma}{\mathrm{d}\Omega_2} = \frac{\mathrm{d}\sigma}{\mathrm{d}\Omega^*} \, 4\cos\alpha \qquad (\alpha < \tfrac{1}{2}\pi). \tag{7.34}$$

In the particular case of equal-mass hard spheres, this differential cross-section has exactly the same form as (7.32). This shows that in the scattering of identical hard spheres the numbers of scattered particles and recoiling target particles entering the detector are precisely equal, and the total detection rate is obtained by doubling that found earlier.

7.5 Summary

For our later work, the most important result of this chapter is that the total momentum, angular momentum and kinetic energy in an arbitrary frame differ from those in the CM frame by an amount equal to the contribution of a particle of mass M moving with the centre of mass.

We have seen that for a two-particle system the use of the CM frame is often a considerable simplification, and this is true also for more complicated systems. When we need results in some other frame, it is often best to solve the problem first in the CM frame, and then transform to the required frame. This is true for example in the calculation of scattering cross-sections in two-particle collisions.

it is $22\,\mathrm{km\,s^{-1}}$, if the deceleration on re-entry into the atmosphere is to be produced by the rockets rather than atmospheric friction.

8.2 Angular Momentum; Central Internal Forces

The total angular momentum of our system of particles is

$$\boldsymbol{J} = \sum_i m_i \boldsymbol{r}_i \wedge \dot{\boldsymbol{r}}_i. \tag{8.11}$$

The rate of change of $\boldsymbol{J}$ is

$$\dot{\boldsymbol{J}} = \sum_i m_i \boldsymbol{r}_i \wedge \ddot{\boldsymbol{r}}_i = \sum_i \sum_j \boldsymbol{r}_i \wedge \boldsymbol{F}_{ij} + \sum_i \boldsymbol{r}_i \wedge \boldsymbol{F}_i. \tag{8.12}$$

Now let us examine the contribution to (8.12) from the internal force between a particular pair of particles, say 1 and 2. (See Fig. 8.2.) For simplicity, let us write $\boldsymbol{r} = \boldsymbol{r}_1 - \boldsymbol{r}_2$, and $\boldsymbol{F} = \boldsymbol{F}_{12}$, so that also $\boldsymbol{F}_{21} = -\boldsymbol{F}$.

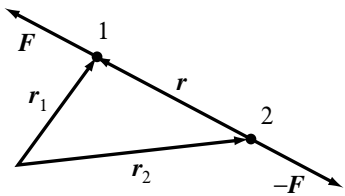

Fig. 8.2

The contribution consists of two terms,

$$\boldsymbol{r}_1 \wedge \boldsymbol{F}_{12} + \boldsymbol{r}_2 \wedge \boldsymbol{F}_{21} = \boldsymbol{r}_1 \wedge \boldsymbol{F} - \boldsymbol{r}_2 \wedge \boldsymbol{F} = \boldsymbol{r} \wedge \boldsymbol{F}. \tag{8.13}$$

This contribution will be zero if $\boldsymbol{F}$ is a *central* internal force, parallel to $\boldsymbol{r}$.

Let us for the moment simply *assume* that all the internal forces are central. (We shall discuss the possible justification for this assumption shortly.) Then all the terms in the double sum in (8.12) will cancel in pairs, just as they did in the evaluation of the rate of change of total linear momentum. The total moment of all the internal forces will be

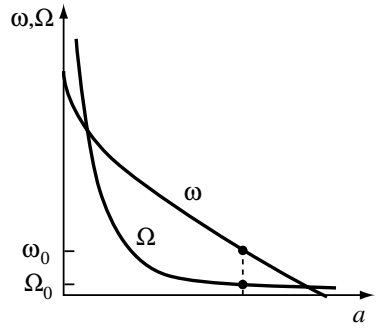

Fig. 8.4

It is important to note that if at any time Ω were actually larger than ω, so that the Moon revolved around the Earth in less than a day, then the tidal forces would act to *increase* the angular velocities and *decrease* the separation. On this simple picture, the smallest distance there can have been between the bodies corresponds to the first point where the curves cross (about 2.3 Earth radii, with a common rotation period of under 5 hours). However, it is in fact impossible that the Moon should ever have been so close, because it would then have been inside the *Roche limit* (about 2.9 Earth radii) where the tidal forces become so strong that they would break up the Moon (see Chapter 6, Problem 20). It is now generally believed that the material that later formed the Moon was ejected from a proto-Earth in a violent collision with another planet early in its history, and then gradually condensed into the present Moon in an orbit with a radius of a few Earth radii.

The final state of the system in the very distant future would correspond to the second point where the curves cross. Then ω and Ω would again be equal, and tidal forces would play no further role. In this final state, the Earth would always present the same face to the Moon, as the Moon already does to the Earth (except for a small wobble). The distance between Earth and Moon would then be about half as large again as it now is, and the common rotation period (the 'day' or the 'month') would be nearly 48 days.

There are, however, several factors which might modify this picture. It was at one time believed that Mercury and the Sun had reached the final state described above, and that Mercury always presents the same face to the Sun. However, it is now known that the ratio of the orbital

We shall see later that these two equations are sufficient to determine the motion completely.

One very important application of (9.1) and (9.2) should be noted. For a rigid body at rest, $\dot{\boldsymbol{r}} = \boldsymbol{0}$ for every particle, and thus both $\boldsymbol{P}$ and $\boldsymbol{J}$ vanish. Clearly, the body can remain at rest only if the right hand sides of both (9.1) and (9.2) vanish, *i.e.*, if the sum of the forces and the sum of their moments are both zero. In fact, as we shall see, this is not only a necessary, but also a sufficient, condition for equilibrium.

Under the same assumption of central internal forces, we saw in §8.5 that the internal forces do no work, so that

$$\dot{T} = \sum \dot{\boldsymbol{r}} \cdot \boldsymbol{F}. \tag{9.3}$$

This might at first sight appear to be a third independent equation. However, we shall see later that it is actually a consequence of the other two. It is of course particularly useful in the case when the external forces are conservative, since it then leads to the conservation law

$$T + V = E = \text{constant}, \tag{9.4}$$

where V is the *external* potential energy, previously denoted by V_{ext}. (Note that there is no mention here of internal potential energy; in a rigid body, this does not change.)

The assumption that the internal forces are central is much stronger than it need be. Indeed, as we discussed in §8.3, it could not be justified from our knowledge of the internal forces in real solids, which are certainly not exclusively central, and in any case cannot be adequately described by classical mechanics. All we actually require is the validity of the basic equations (9.1) and (9.2), and it is better to regard these as basic assumptions of rigid body dynamics, whose justification lies in the fact that their consequences agree with observation. To some extent, the success of these postulates, particularly (9.2), may seem rather fortuitous. However, we shall see in Chapter 12 that it is closely related to the relativity principle discussed in Chapter 1.

9.2 Rotation about an Axis

Let us now apply these basic equations to a rigid body which is free to rotate only about a fixed axis, which for simplicity we take to be the z-axis.

in general it depends in a more complicated way on the co-ordinates themselves:

$$\dot{\boldsymbol{r}}_i = \sum_{\alpha=1}^{n} \frac{\partial \boldsymbol{r}_i}{\partial q_\alpha} \dot{q}_\alpha + \frac{\partial \boldsymbol{r}_i}{\partial t}.$$

The last term arises from the explicit dependence on t in (10.1), and is absent for a natural system. When we substitute in $T = \sum \frac{1}{2} m \dot{\boldsymbol{r}}^2$, we obtain a quadratic function of the time derivatives $\dot{q}_1, \ldots, \dot{q}_n$. For a natural system, it is a *homogeneous* quadratic function; but for a forced system there are also linear terms and terms independent of the velocities.

For example, according to (8.29) and (9.46), the kinetic energy of a symmetric rigid body is

$$T = \tfrac{1}{2} M(\dot{X}^2 + \dot{Y}^2 + \dot{Z}^2) + \tfrac{1}{2} I_1^* (\dot{\varphi}^2 \sin^2\theta + \dot{\theta}^2) + \tfrac{1}{2} I_3^* (\dot{\psi} + \dot{\varphi}\cos\theta)^2.$$

If we impose further algebraic constraints, such as $X = 0$, the corresponding terms drop out, and we are still left with a homogeneous quadratic function of the remaining time derivatives. On the other hand, if we impose a differential constraint, such as $\dot{X} = u$ or $\dot{\varphi} = \omega$, we obtain a function with constant or linear terms.

10.2 Lagrange's Equations

To obtain a more general form of Lagrange's equations than the one found in §3.7 — in particular, one that is not restricted to conservative forces — let us return for the moment to the case of a single particle, moving under an arbitrary force $\boldsymbol{F}$. We consider variations of the integral

$$I = \int_{t_0}^{t_1} T \,\mathrm{d}t, \qquad \text{where} \qquad T = \tfrac{1}{2} m \dot{\boldsymbol{r}}^2. \tag{10.2}$$

Now let us make a small variation $\delta x(t)$ in the x co-ordinate, subject to the boundary conditions $\delta x(t_0) = \delta x(t_1) = 0$. Then clearly $\delta T = m\dot{x}\,\delta\dot{x}$. Substituting in (10.2), and performing an integration by parts, in which the integrated term vanishes by virtue of the boundary conditions, we find

$$\delta I = -\int_{t_0}^{t_1} m\ddot{x}\,\delta x \,\mathrm{d}t.$$

Now, the integrand is $-F_x\,\delta x = -\delta W$, where δW is the work done by the force $\boldsymbol{F}$ in the displacement δx. Similarly, if we make variations of all three

fields $\boldsymbol{v}_j$ allow us to define a co-ordinate grid continuously over the surface $\boldsymbol{M}$ and without any singularity. The topology of $\boldsymbol{M}$ is then necessarily that of a *torus* — an n-dimensional 'ring doughnut' embedded within the full $2n$-dimensional phase space.

For a system of one degree of freedom each $\boldsymbol{M}$ is a 1-torus $F_1 \equiv H =$ constant, *i.e.* a one dimensional loop in the two-dimensional phase space. (See Fig. 14.1(a).) Evidently $\boldsymbol{v}_1$ here is tangent to the curve at each point of $\boldsymbol{M}$. For different values of F_1 we obtain different loops $\boldsymbol{M}$, members of a set of 'nested' tori, as for example in Fig. 13.4.

For a system of two degrees of freedom each $\boldsymbol{M}$ is a 2-torus, *i.e.* a two-dimensional 'ring doughnut' surface embedded in the four-dimensional phase space. (See Fig. 14.1(b).) In this case we can take $\boldsymbol{v}_1, \boldsymbol{v}_2$ everywhere parallel to distinct loops which can parametrize the surface. It is the case that $\boldsymbol{M}$ cannot have, for example, the topology of a sphere, because all $\boldsymbol{v}_1, \boldsymbol{v}_2$ parametrizations of such a surface are necessarily singular, at least somewhere. In Fig. 14.1(c) the attempt to use a grid of lines of latitude and longitude is singular at the poles. That all such attempts for a sphere are bound to be singular is a consequence of the 'hairy ball theorem' of topology; this theorem also implies, among other things, the existence of at least one crown parting in the combing of a head of hair, and that a spherical magnetic bottle *must* leak!

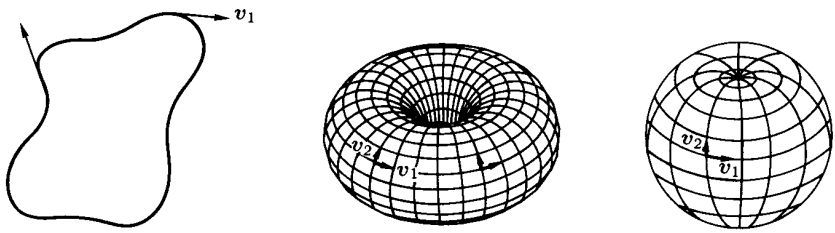

Fig. 14.1

The n-tori for an integrable system of n degrees of freedom in its $2n$-dimensional phase space are often called *invariant tori* because a trajectory (orbit) which is initially on one of them ($\boldsymbol{M}$) remains on it for ever. Different initial conditions then lead to tori which are nested within the phase space.

so that the eigenvalues are $\lambda_1 = 1, \lambda_2 = -1$ with eigenvectors

$$\begin{bmatrix} 1 \\ 0 \end{bmatrix}, \quad \begin{bmatrix} 0 \\ 1 \end{bmatrix}$$

respectively. The trajectories near the origin, which is a *saddle*, are indicated in Fig. C.8(a). For the exact nonlinear system (C.10) we can write

$$\frac{\mathrm{d}y}{\mathrm{d}x} = -\frac{y}{x} + x, \tag{C.11}$$

so that

$$y = \frac{x^2}{3} + \frac{c}{x}, \qquad \text{with } c \text{ constant},$$

together with a second solution $x = 0$ (for all y).

The exact family of trajectories near the origin is indicated in Fig. C.8(b). It should be noted that the trajectories which go directly into and directly out of the critical point O (respectively the stable and unstable manifolds) correspond directly at and near O for the exactly linear and almost linear systems — a general result usually known as the *stable manifold theorem*.

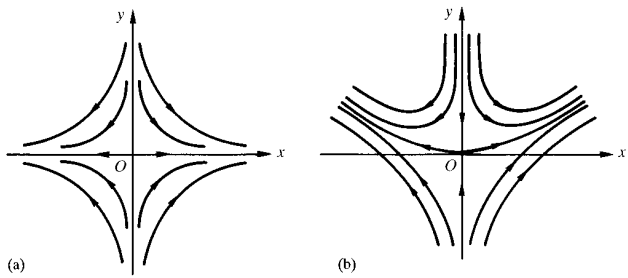

Fig. C.8

C.3 Systems of Third (and Higher) Order

As we indicated in §13.6, higher-order systems can be analyzed in a similar fashion to that carried out in §13.3 and earlier in this appendix. That is to say the critical points are found and local analysis effected about each of

2.8 Impulsive Forces; the Green's Function Method

There are many physical situations, for example collisions, in which very large forces act for very short times. Let us consider a force F acting on a particle during the time interval Δt. The resulting change of momentum of the particles is

$$\Delta p = p(t + \Delta t) - p(t) = \int_t^{t+\Delta t} F \, \mathrm{d}t. \tag{2.50}$$

The quantity on the right is called the *impulse* I delivered to the particle. It is natural to consider an idealized situation in which the time interval Δt tends to zero, and the whole of the impulse I is delivered to the particle instantaneously. In other words, we let $\Delta t \to 0$ and $F \to \infty$ in such a way that the impulse I remains finite. At the instant when the impulse is delivered the momentum of the particle changes discontinuously. Although in reality the force must always remain finite, this is a good description of, for example, the effect of a sudden blow.

In the next section, we shall discuss some simple collision problems. Here, we shall consider the effect of an impulsive force on an oscillator. Let us suppose first that the oscillator is at rest at its equilibrium position $x = 0$, and that at time $t = 0$ it experiences a blow of impulse I. Immediately after the blow, its position is still $x = 0$ (since the velocity remains finite, the position does not change discontinuously), while its velocity is $v_0 = I/m$. Inserting these initial conditions in the general solution (2.31) for the oscillatory case $\gamma < \omega_0$, we find that the position is given by

$$x = \begin{cases} 0, & t < 0, \\ \dfrac{I}{m\omega} \mathrm{e}^{-\gamma t} \sin \omega t, & t > 0. \end{cases} \tag{2.51}$$

This solution is illustrated in Fig. 2.9.

Just as in the case of periodic forces, we can immediately generalize this result to a sum of impulsive forces. If the oscillator is subjected to a series of blows, of impulse I_r at time t_r, its position may be found by adding together the corresponding set of solutions of the form (2.51). We obtain in this way

$$x(t) = \sum_r G(t - t_r) I_r + \text{transient}, \tag{2.52}$$